

Numerical analysis and fluid-solid coupling model test of filling-type fracture water inrush and mud gush

Li-Ping Li^{1,3a}, Di-Yang Chen^{1,2b}, Shu-Cai Li^{1a}, Shao-Shuai Shi^{*1},
Ming-Guang Zhang^{4a} and Hong-Liang Liu^{1b}

¹Research Center of Geotechnical and Structural Engineering, Shandong University, Jinan, China

²Research Institute of New material and intelligent equipment, Shandong University, Dezhou, China

³State Key Lab of Subtropical Building Science, South China University of Technology, Guangzhou, China

⁴College of Mining and Safety Engineering, Shandong University of Science and Technology, Qingdao, China

(Received January 11, 2016, Revised March 21, 2017, Accepted July 5, 2017)

Abstract. The geological conditions surrounding the Jijiapo Tunnel of the Three Gorges Fanba Highway project in Hubei Province are very complex. In this paper, a 3-D physical model was carried out to study the evolution process of filling-type fracture water inrush and mud gush based on the conditions of the section located between 16.040 km and 16.042 km of the Jijiapo Tunnel. The 3-D physical model was conducted to clarify the effect of the self-weight of the groundwater level and tunnel excavation during water inrush and mud gush. The results of the displacement, stress and seepage pressure of fracture and surrounding rock in the physical model were analyzed. In the physical model the results of the model test show that the rock displacement suddenly jumped after sustainable growth, rock stress and rock seepage suddenly decreased after continuous growth before water inrushing. Once water inrush occurred, internal displacement of filler increased successively from bottom up, stress and seepage pressure of filler dropped successively from bottom up, which presented as water inrush and mud gush of filling-type fracture was a evolving process from bottom up. The numerical study was compared with the model test to demonstrate the effectiveness and accuracy of the results of the model test.

Keywords: filling-type fracture; water inrush and mud gush; model test; numerical modeling; evolution law.complex terrain

1. Introduction

Water inrush and mud gush greatly endangers the safety of tunnel construction. Hundreds of water inrush disasters have occurred over last fifty years in China and elsewhere, resulting in huge casualties and property losses (Li *et al.* 2010, Li *et al.* 2013). The natural rock fractures generally contain filler medium, the original rock broken things of engineering rock mass fill in the fracture (Lomize 1951). There are obvious differences in the seepage law of rock fracture with or without

*Corresponding author, Ph.D., E-mail: sss_sdu@163.com

^aPh.D

^bPh.D Student

material (Liu *et al.* 2010). It is essential to research mechanism of filling-type fracture water inrush and mud gush and take some effective countermeasures to assure the safety of tunnel construction. A great number of researches have been conducted to analyze the seepage characteristic of filling-type fracture. Liu *et al.* (2002) investigated the seepage law of rock fractures in combination with sand property based on shear-seepage test. Wang *et al.* (2008) carried out an experiment equipment to assess the effect of the hydraulic conductivity of surrounding rock on the water pressure on lining. Liu *et al.* (2012) proposed the non-symmetric sinusoidal fracture model to simulate the flow in a real fracture. Kiyoshi *et al.* (2012) carried out a 2-D model test to capture the mechanism of fracture seepage flow considering the inhomogeneous structure of single rock fractures.

Numerical modeling using the finite element and the finite difference schemes can analyze the tunnel water inrush problems in various complicated geological conditions (Hwang and Lu 2007, Lia *et al.* 2013). Wang *et al.* (2002) and Noghabai (1999) established the seepage-damage model of rock during the process of water inrush. Model testing is often used to simulate the water inrush, and a lot of research works on the water inrush mechanism have been conducted. Zhang (2004) discussed the potential water inrush disasters from aquifers under coal seams. Nevertheless, little is studied at present about the problem on the water inrush and mud gush of filling-type fracture.

As discussed previously, 3-D physical model tests and numerical calculations of tunnels are the two important methods to investigate the characteristics of water inrush and mud gush during tunneling. In this paper, a 3-D physical model test was carried out to investigate the water inrush and mud gush for the case of Jijiapo Tunnel. Moreover, a 3-D numerical analysis was also carried out using the software FLAC3D. Some beneficial phenomenon and conclusion were obtained from the stress field, displacement field and seepage field of filling-type fracture and surrounding rock, and preliminarily reveal the instability mechanism of the fracture filler. These results may provide valuable guidance for the construction of this type of tunnel throughout the world.

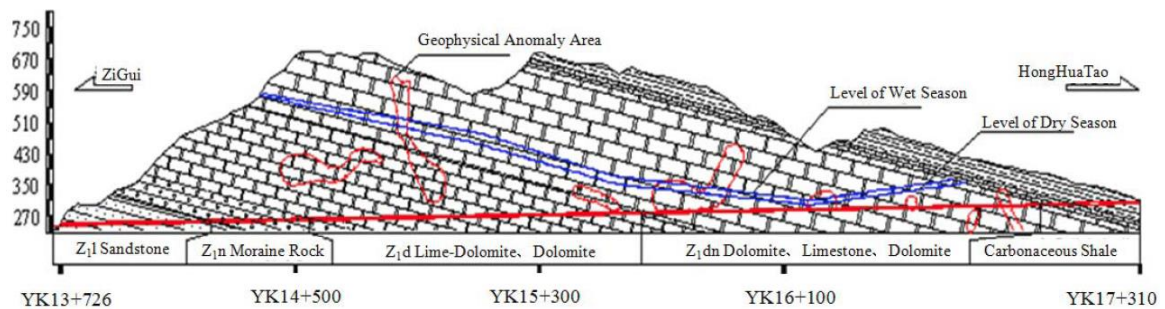


Fig. 1 Engineering geology of Jijiapo tunnel

Table 1 Grain size analysis of the karst fracture's filler

Particle	Particle Size (mm)	Description
Gravel grain	$2 < d \leq 60$	The sediment contains gravel grain, poor roundness and sorting, the main gravel grain is fine gravel
Silt and sand grain	$0.005 < d \leq 2$	Yellow-white, white is dominant, there are two sources: The first one is sandstone of dolomite, and the second one is river sand
Clay	$d \leq 0.005$	Dark brown, its formation is black soil of gully and high wall, and red clay filled in solution crack

2. Engineering background

Jijiapo Tunnel was probably the most significant engineering feature of Three Gorges Fanba Highway project, which is located in the typical karst areas in Hubei Province, central China. Jijiapo Tunnel is 3.4 km long, with a maximum overburden thickness of 390 m. The main geologic formation crossed by the Jijiapo Tunnel is shale, moraine rock, sandstone, limestone, carbonaceous shale and dolomitic limestone. The length of left tube is 3363 m (ZK13+835-ZK17+835) and right tube is 3463 m (YK13+757-YK17+757). The engineering geological cross section of Jijiapo Tunnel is presented in Fig. 1.

The main aquifers pass through by the Jijiapo Tunnel include a strong karst aquifer from ZK15+938 to ZK16+086. The high-step-tilt water-storing structure of karst fracture was exposed during the tunnel excavation between YK16+040 and YK16+042. The fracture intersects with the tunnel axis at a small angle (about 20°). The fracture trace length is greater than 20 m, and the occurrence of fracture is 30°~70°. The visible width of fracture in tunnel is 20-40 cm, extend upward. The width of fracture after extended upward is assumed to be 0.3-3 m based on the character of filler. The fracture is developed into a high-angle karst cave, and the cavity was packed with particle. The size grading of sediment is divided into three categories, which is shown in Table 1.

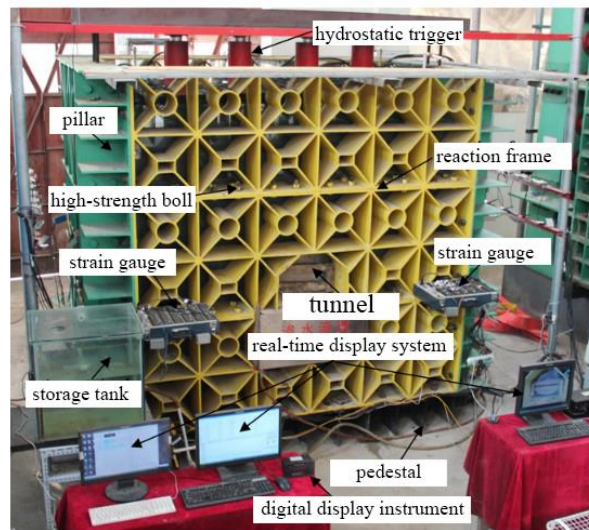


Fig. 2 Photograph of structural steel frame for 3-D model test

Table 2 Proportion of similar material (mass unit)

Material	Simulated rock	Simulated filler
Material proportion of compositions	S:I:C:P:O=1.0:1.2:0.2:0.25:0.13	S:Cl:C:P:O=1.0:0.8:0.14:0.24:0.11
Molar concentration of cementing agent	18%	14%
Proportion of cementing agent	12%	8%

*Note: S, sand; I, iron powder; C, cement; P, chlorinated paraffin; O, silicone oil; Cl, clay

3. Physical model

3.1 Steel frame

A test equipment is developed to simulate the filling-type fracture water inrush and mud gush in tunnel engineering. The photograph of steel structural frame in our work for the 3-D model tests is shown in Fig. 2. The frame accommodated the model and served as a reaction device for loading. The frame consisted of a base, a layered reaction frame, structural walls, loading jacks and combination walls. The pillars, pedestals and reaction frames were connected by high-strength bolts. To reinforce the visualization and strength of the structure, the high-strength toughened glass was applied in the steel frame. The dimensions (length×width×height) of test bench are adopted as 3.0 m×1.8 m×2.7 m.

3.2 Model material

The simulated rock was mixed with sand, calcium carbonate, iron powder, cement, chlorinated paraffin and silicone oil, and the simulated filler was composed of sand, clay, white cement, chlorinated paraffin and silicone oil. The combination ratio of these materials was determined based on the results of uniaxial compression tests and falling head permeability tests, as shown in Table 2. Figs. 3-5 present the influence of the contents of these compositions on the behavior of the simulated rock. The parameters of the model material are derived based on the law of similitude (Li 2009, Huang *et al.* 2012). The proportion of the two materials is obtained according to the experiment results. Table 3 shows the mechanical parameters of the model material.

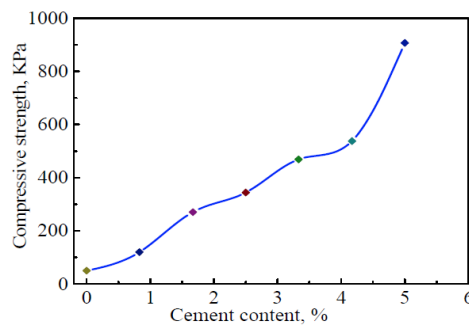


Fig. 3 Influence of the contents of quartz sand and barite powder on the compression strength

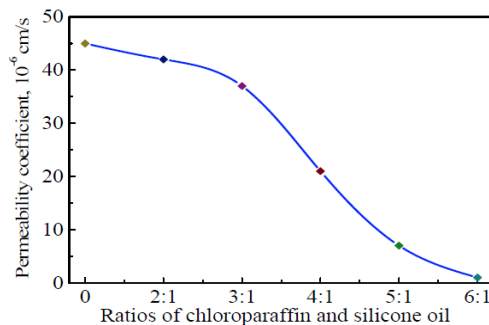


Fig. 4 Influence curves of cement content and ratios of silicone oil on permeability coefficient of material

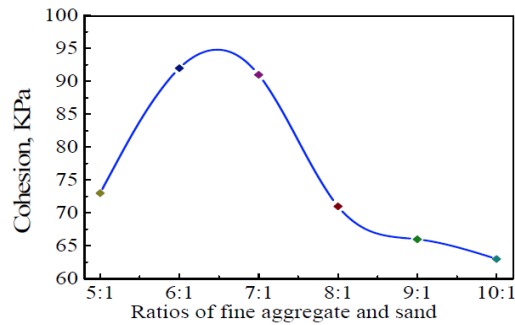


Fig. 5 Influence of the contents of alcohol rosin solution and iron powder on the cohesion

Table 3 Mechanical parameters of model materials

	Simulated rock	Simulated filler
Bulk density (KN·m-3)	26.6	15
Elastic modulus(MPa)	98	34
Poisson ratio	0.15	0.30
Cohesion (kPa)	0.10	0.05
Friction angle (°)	32	13
Compressive strength (MPa)	0.8	0.3
Permeability Coefficient (cm·s-1)	1.24×10^{-5}	5.49×10^{-4}

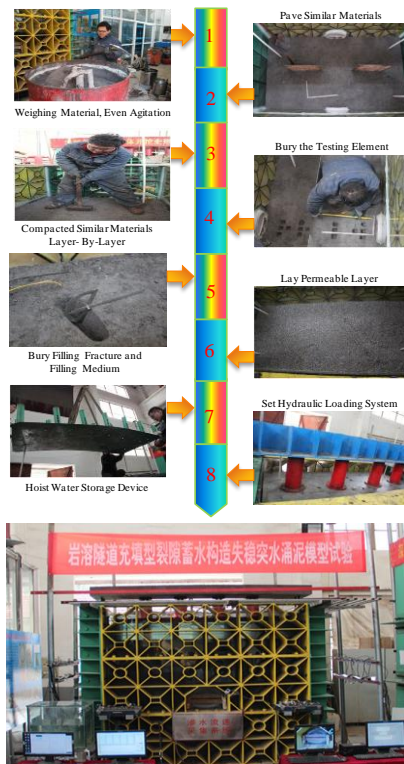


Fig. 6 The basic process of model body formation

3.3 Model body formation

In order to assess to the effect of the water inrush channel formation in the filling-type fracture during the tunnel excavation, the filling-type fracture was placed at a dip angle of 30° according to the geological conditions of the tunnel. The material was filled layer-by-layer to simulate the fractures. After a layer of the material had been air-dried, the subsequent layer of the material was then applied. Therefore, there would be an interface between two layers. The process of model body formation is shown in Fig. 6.

3.4 Measurement of model deformation

To measure multivariate information (such as displacement, seepage pressure, stress and strain) during the tunnel excavation, a number of fiber optic osmometers, multi-point extensometers, resistance strain gauges and micro pressure-cells were installed in the model during its construction. The photo of the micro pressure-cell and fiber optic osmometer is shown in Fig. 7. There are two monitoring sections: Monitoring Section I and Monitoring Section II. The location of the monitoring elements is shown in Fig. 8.



Fig. 7 Layout of monitoring elements

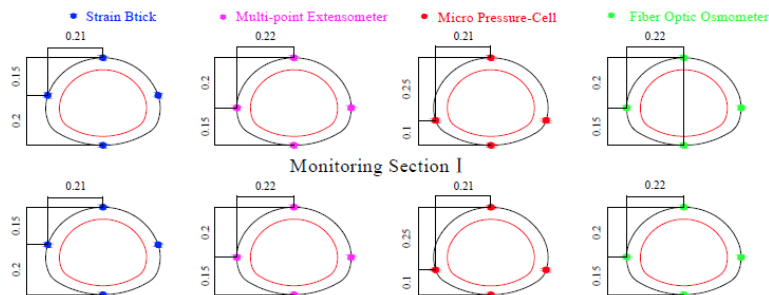


Fig. 8 The location of monitoring elements

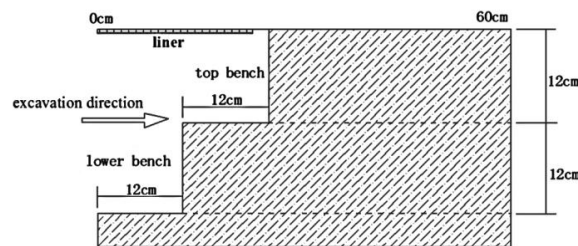


Fig. 9 Excavation schematic diagram



Fig. 10 Excavation in Tunnel



Fig. 11 Inflow of water and mud in Tunnel

3.5 Simulation of the construction process in the model test

The similarity ratio of the model was selected as 1:35. The dimensions (length×width×height) of the visualization fluid-solid coupling laboratory were 2.4 m×1.2 m×2.4 m. The direction of length was vertical with the axes of the tunnel and the direction of width parallel with the axes of the tunnel. The tunnel section was separated into two benches. Lengthwise excavation was divided into 20 steps with each 3-cm-long step. The length of top bench was designed to be 12 cm. After the top bench was excavated for four steps, the lower bench began to be excavated together with the top bench. Excavation schematic diagram is shown in Figs. 9 and 10. The support patterns of the section were liners. Inflow of water and mud in tunnel is shown in Fig. 11.

4. Numerical simulation of construction

4.1 Numerical model and boundary conditions

The material behavior was assumed to be governed by an elastic-plastic constitutive model based on the Mohr-Coulomb failure criterion. Based on the engineering geological data obtained from the site tests of the Jijiapo Tunnel, a 3-D numerical model was created using ANSYS. The 3-D numerical model was created using ANSYS and then transferred to FLAC 3D using the ANSYS-FLAC interface program. The horizontal direction (X direction), vertical direction (Y coordinate) and axial direction (Z coordinate) were adopted as 84 m in length, 21 m in height and 63 m in length, respectively. The height of internal fracture was 21 m, the width of fracture was 1.75 m in the lower and 3.5 m in the upper. The origin of the coordinates was assumed to be located at the tunnel crown. In the model, 252,423 tetrahedron elements were used. In the four side surfaces only the normal displacements were constrained, and in the bottom surface all these

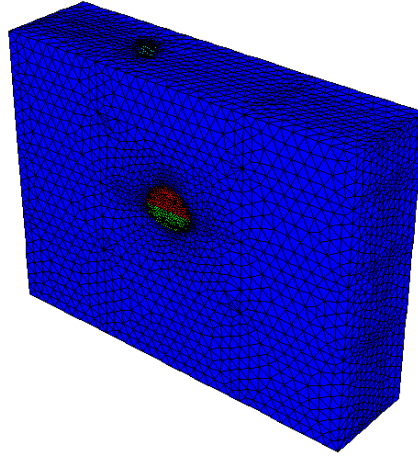


Fig. 12 Numerical grid of the 3-D model

Table 4 Physico-mechanical parameters

Material	Simulated rock	Simulated filler
Bulk density (KN m ⁻³)	26.6	15
Elastic modulus(GPa)	2.4	0.8
Poisson ratio	0.15	0.30
Cohesion (kPa)	0.6	0.2
Friction angle (°)	32	13
Compressive strength (MPa)	31	15
Permeability Coefficient (cm s ⁻¹)	1.87×e ⁻⁵	1.23×e ⁻⁴

displacement directions were constrained. Fig. 12 shows the numerical grid used for simulation the model.

4.2 Initial ground stresses and initial seepage field

The initial ground stress in vertical direction was the stress due to the self-weight of the rock. The horizontal stress was adopted as 0.76 times vertical stress according to the geological investigation report. The overburden depth for the model tunnel was assumed to be 390 m. A load was applied to the top surface of the numerical model to simulate the actual heights. The initial seepage field in vertical direction was the water stress due to the self-weight of the groundwater level. The groundwater level depth for the model tunnel was assumed to be 100 m. A load was also applied to the top surface of the numerical model to simulate the actual heights of groundwater level.

4.3 Physical-mechanical parameters

Many laboratory tests of the limestone of Jijiapo Tunnel and the filler of fracture located between YK16+040 and YK16+042 were conducted including uniaxial compression tests, triaxial

compression tests, triaxial rheological tests and falling head permeability test. For consistency all of the specimens were kept in their fully saturated condition. The required physical-mechanical parameters of the interface are shown in Table 4.

5. Analysis of model test results

During the tunnel excavating process, the mechanical state of filling-type fracture and surrounding rock changed continuously, which was pregnant with precursor information of water inrush and mud gush. The catastrophe evolution process of filler was analyzed in the present paper by real-time monitoring the stress and displacement of monitoring-points. The arrangement plan of monitoring-points is shown in Fig. 13.

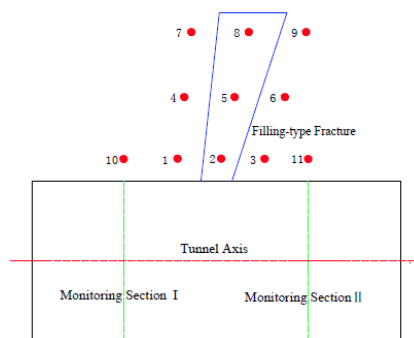


Fig. 13 Schematic diagram of monitoring-point for seepage pressure, displacement and so on

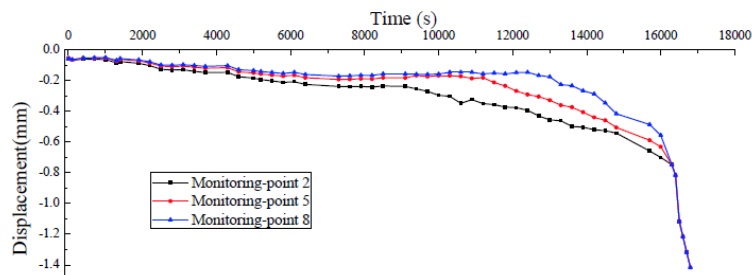


Fig. 14 Time-history curve of displacement for monitoring-points

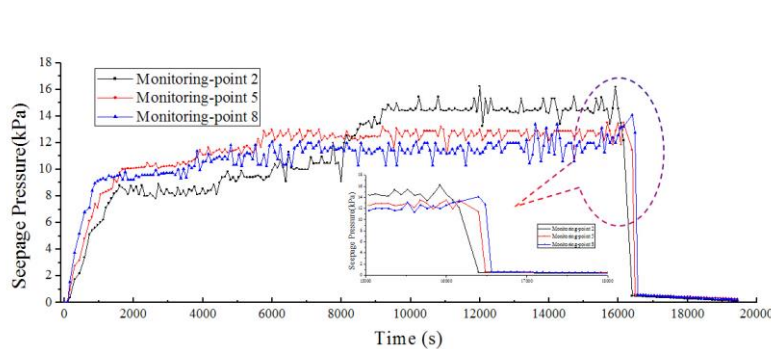


Fig. 15 Time-history curve of seepage pressure for the monitoring-points

5.1 Displacement analysis of fracture

Fig. 14 shows the time-history curve of displacement for monitoring-point 2, monitoring-point 5 and monitoring-point 8 (the arrangement plan of three monitoring-points is shown in Fig. 13). Before 1000 s, the displacement of three monitoring-points changed mildly with the passage of time. The displacement of monitoring-point 2 increased when excavation face passed through the lower part of fracture (9500 s). At 11000 s, the displacement of the monitoring-points 5 and 8 showed an increase tendency. As time gone by (12000 s to 14000 s), the displacement of three monitoring-points significantly increased. The displacement of three monitoring-points had a distinct “plunge” point, which presented as water inrush and mud gush took place at about 16000 s.

5.2 Seepage pressure analysis of fracture

Fig. 15 shows time-history curve of seepage pressure for monitoring-point 2, monitoring-point 5 and monitoring-point 8. Initial seepage pressure field was formed rapidly at the early days of tunnel excavation (0 s-1000 s), and the seepage pressure of three monitoring-points increased from 1000 s to 6000 s, which manifested as water inrush channel of fracture expand primary. The seepage pressure of the three monitoring-points was involved in a relatively stable stage at 6000 s-8000 s, while the small amplitude explosion segments appeared after 8000 s. The seepage pressure of the monitoring-point 5 and 8 still kept at relatively stable stage. After 10000 s, the seepage pressure of the monitoring-point 2 was also involved in a relatively stable stage. Thereafter, the seepage pressure of the three monitoring-points was lager from 12000 s and 14000 s, which mainly manifested as the relatively large-scale water inrush channels preliminarily formed in the fracture filler. The seepage pressure of the three monitoring-points significantly increased at about 16000 s, which presented as water inrush and mud gush occurred at this moment. Therefore, the water inrush and mud were gushed of filling-type fracture manifested as the collectivity sudden jump of seepage pressure of filler.

5.3 Displacement analysis of monitoring section

Fig. 16 shows the time-history curve of displacement for monitoring-point 10 (Monitoring Section I) and monitoring-point 11 (Monitoring Section II). The surrounding rock displacement of

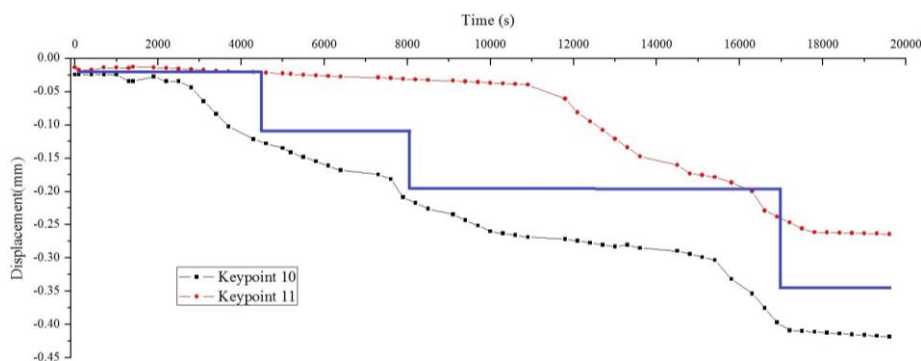


Fig. 16 Time-history curve of displacement for monitoring-points

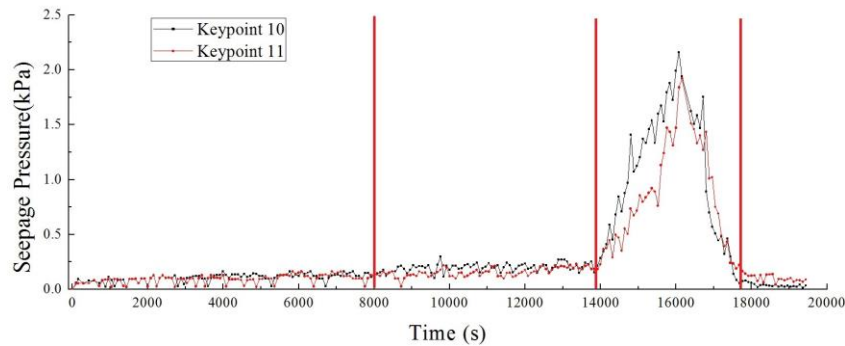


Fig. 17 Time-history curve of seepage pressure for monitoring-points

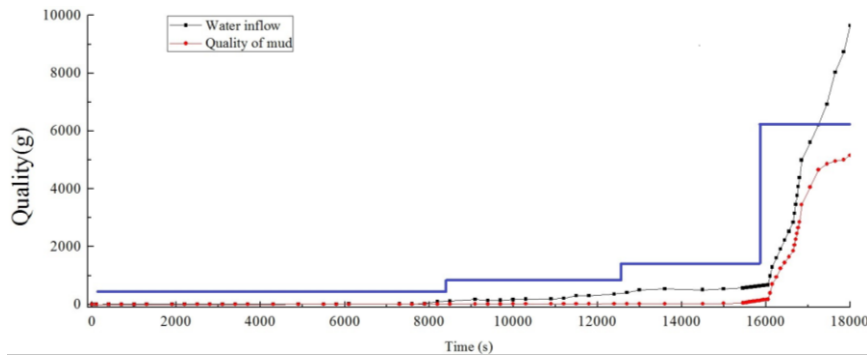


Fig. 18 Time-history curve of water inrush and mud gush quantity

two monitoring-points was relatively small, deformation and deformation rate increased with the passage of time. The displacement rate of monitoring-point 10 increased at about 3000 s, while the tunnel was excavated through the Monitoring Section I, and increased continuously at 3000 s-10000 s. However, the change rate of deformation was smaller at 10000 s-12000 s. The displacement rate of monitoring-point 11 was relatively small at 0 s-9000 s. The displacement rate increased in small range at 10000 s-12000 s. The displacement rate increased obviously after 12000 s, the tunnel was excavated through the Monitoring Section II. The displacement of two monitoring-points increased at small amplitude at about 16000 s. Subsequently, the displacement tended to be stable.

5.4 Seepage pressure analysis of monitoring section

Fig. 17 shows the time-history curve of seepage pressure for monitoring-point 10 (Monitoring Section I) and monitoring-point 11 (Monitoring Section II). Before 14000 s, the seepage pressure was small. At 14000 s, the seepage pressure increased sharply, and reached the peak (about 2.0 kPa) at 16000 s. Thereafter, the seepage pressure decreased sharply. After 16000 s, the reason of the sudden drawdown of seepage pressure value was water inrush occurred at this moment.

5.5 Analysis of water irruption quantity

Fig. 18 shows the time-history curve of water inrush and mud gush quantity. From initial

excavating period to 10000 s, there were insignificantly water intruding and mud gushing, which presented as the seepage water occurred. At 12500 s, seepage water phenomenon intensifies, water intrush channel was formed, and the water was associated with a little sediment. The diameter of channel larger, at 13000 s. Water intrush and mud gush quantity significantly increased at 14000 s. The filler was flushed out of fracture at 16000 s, the inflow of water increased continuously, which presented as the channels formed.

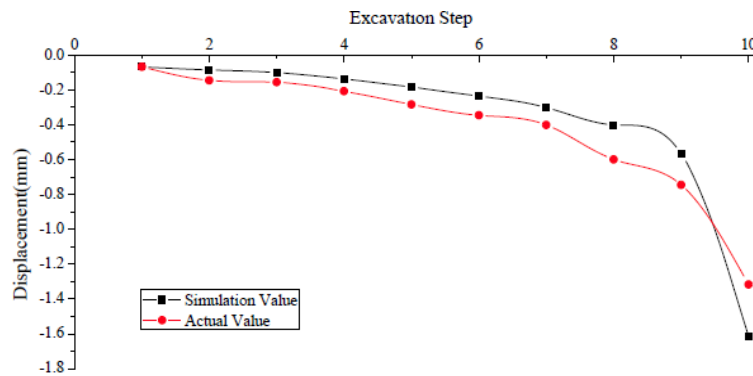


Fig. 19 Displacement comparison curve of monitoring-point 2

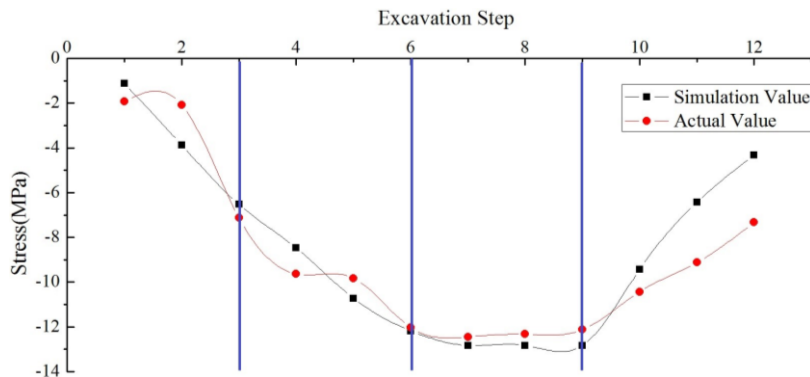


Fig. 20 Stress comparison curve of monitoring-point 2

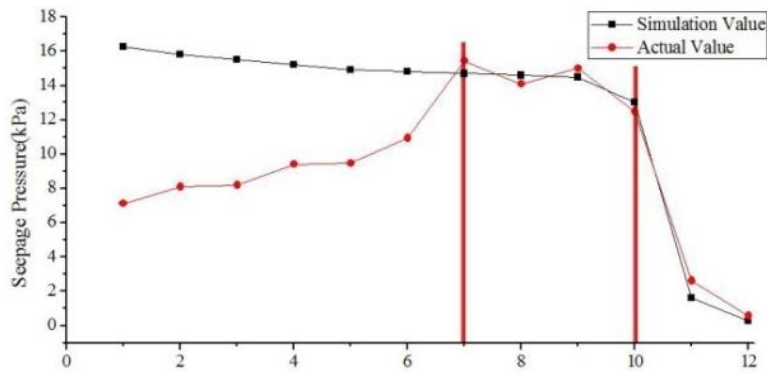


Fig. 21 Seepage-pressure comparison curve of monitoring-point 2

6. Comparison of physical and numerical model results

Because the similarity ratio of the model was selected as 1:35, the dimensions of the numerical model are 35 times that of the physical model.

6.1 Comparative analysis of displacement information

Fig. 19 shows the displacement comparison curve of monitoring-point 2. The deformation of filler was small at the early days of tunnel excavation. The deformation of filler increased by a small margin after the second excavation step, the displacement rate was obviously larger after the seventh excavation step. There was water leakage out of the bottom near the fracture and side wall, and there was water point with larger area at local. The filler was gushed out suddenly at the tenth excavation step, which presented as the water inrush channels formed.

6.2 Comparative analysis of stress information

Fig. 20 shows the stress comparison curve of monitoring-point 2. The vertical stress of filler firstly increased and then decreased. The vertical stress was thought to be a line procedure after the sixth excavation step, than after the ninth excavation step, the vertical stress was thought to be a quickly falling stage. The filler was collapsed sustainability, and gushed completely.

6.3 Comparative analysis of seepage pressure

Fig. 21 shows the seepage-pressure comparison curve of monitoring-point 2. Initial stable seepage pressure field was formed rapidly, the deformation of filler decreased in a small margin at the early days of tunnel excavation, the surrounding rock stress entered into an adjustment period. At the last half way, the change of seepage pressure was relatively flat. After the ninth excavation step, the value of seepage pressure had wide flounce range. The filler was gushed suddenly at the tenth excavation step, which presented as the water inrush channels formed.

7. Conclusions

A 3-D physical model test and numerical calculations were carried out to investigate the evolution process of water inrush and mud gush for the case of Jijiapo Tunnel. This paper reveals the response pattern of precursory multi-physics field information of the filling-type fracture water inrush and mud gush. Based on the study above, some important conclusions can be summarized as follows:

- Two new similar materials for fluid-solid coupling were derived based on the law of similitude, one was simulated rock, the other was simulated filler. The simulated rock was mixed with sand, calcium carbonate, iron powder, cement, chlorinated paraffin and silicone oil, and the simulated filler was composed of sand, clay, white cement, chlorinated paraffin and silicone oil.
- The results of the numerical calculations are consistent with those of the model test. The test and numerical results show that under the action of excavation disturbance and high underground water level, water inrush and mud gush process can be divided into the three steps, micro-channels preliminarily form, crack propagation and water gushing passageways transfix. The catastrophe

evolution process for the water inrush and mud gush of filling-type fracture was truly reappeared in this model test.

- During tunnel construction many engineering accidents are closely related to the water inrush and mud gush. Hence, it is important to control the fracture displacements and seepage pressure. This leads to the conclusion that monitoring and prediction of filling-type fracture water inrush and mud gush can start from monitoring multi-variables information of surrounding rock in actual engineering.

Acknowledgments

This research described in this paper was financially supported by the National Natural Science Foundation of China (Grant NO.51679131), the Natural Science Foundation of Shandong Province of China (Grant NO.2014ZRE27303) and the State Key Lab of Subtropical Building Science, South China University of Technology (2016ZB07). The authors would like to express appreciation to the reviewers for their valuable comments and suggestions that helped to improve the quality of the paper.

References

- Huang, H.F., Mao, X.B., Yao, B.H. and Pu, H. (2012), "Numerical simulation on fault water-inrush based on fluid-solid coupling theory", *J. Coal Sci. Eng.*, **18**(3), 291-296.
- Hwang, J.H. and Lu, C.C. (2007), "A semi-analytical method for analyzing the tunnel water inflow", *Tunn. Undergr. Sp. Technol.*, **21**(1), 39-46.
- Kishida, K., Sawada, A., Yasuhara, H. and Hosoda, T. (2012), "Estimation of fracture flow considering the inhomogeneous structure of single rock fractures", *Soils Found.*, **53**(1), 105-116.
- Li, C., Li, J., Li, Z. and Hou, D. (2013), "Establishment of spatiotemporal dynamic model for water inrush spreading processes in underground mining operations", *Safety Sci.*, **55**, 45-52.
- Li, L.P. (2009), "Study on catastrophe evolution mechanism of karst water inrush and its engineering application of high risk karst tunnel", Shandong University, Jinan, China.
- Li, L.P., Li, S.C. and Zhang, Q.S. (2010), "Study of mechanism of water inrush induced by hydraulic fracturing in karst tunnels", *Rock Soil Mech.*, **31**(2) 523-528.
- Li, S.C., Zhou, Z.Q., Li, L.P., Xu, Z.H., Zhang, Q.Q. and Shi, S.S. (2013), "Risk assessment of water inrush in karst tunnels based on attribute synthetic evaluation system", *Tunn. Undergr. Sp. Technol.*, **38**, 50-58.
- Liu, C.H., Chen, C.X. and Fu, S.L. (2002), "Testing study on seepage characteristics of single fracture with sand under shearing displacement", *Chin. J. Rock Mech. Eng.*, **21**(10), 1457-1461.
- Liu, J., Li, J.L. and Wang, R.H. (2010), "Experimental study of seepage in yichang fractured sandstone with tight original rock fillings", *Chin. J. Rock Mech. Eng.*, **29**(2), 367-374.
- Liu, Q.Q. and Fan, H.G. (2012), "The characteristics and estimation of flow through a single rough-walled fracture", *J. Hydrodyn.*, **24**(3), 315-322.
- Lomize, G.M. (1951), *Flow in Fractured Rocks*, Gesenergoizdat, Moscow, Russia.
- Noghabai, K. (1999), "Discrete versus smeared versus element-embedded crack models on ring problem", *J. Eng. Mech.*, **125**(3), 307-315.
- Wang, J.A. and Park, H.D. (2002), "Fluid permeability of sedimentary rocks in a complete stress-strain process", *Eng. Geol.*, **63**(3), 291-300.
- Wang, X., Wang, M., Zhang, M. and Ming, H. (2008), "Theoretical and experimental study of external water pressure on tunnel lining in controlled drainage under high water level", *Tunn. Undergr. Sp.*

Technol., **23**(5), 552-560.

Zhang, J.C. (2004), "Investigations of water inrushes from aquifers under coal seams", *J. Rock. Mech. Min. Sci.*, **42**(3), 350-360.

CC